Theoretical Physics

Boomeron- and Trappon Solitons Investigated Analytically and Numerically

Filip Allard (900314-1232)
filipall@kth.se
David Blomqvist (910315-4614)
davidblo@kth.se
SA104X Degree Project in Engineering Physics, First Level
Department of Theoretical Physics
Royal Institute of Technology (KTH)
Supervisor: Jack Lidmar

May 21, 2013

Abstract

This report presents an analysis of the phenomena of boomeron- and trappon solitons both analytically and numerically. These solitons are investigated in the (1+1) dimension, i.e. one spatial dimension plus the temporal dimension. The investigation regards the Boomeron equation (BE) and the non-linear Schrödinger equation (NLSE). Additional equations giving rise to these phenomena are also presented. A special focus of the investigation is the relation between the changing velocity and the polarization for the BE and the NLSE. For the NLSE, this is enabled through an interpretation of the components for the single-soliton solution.

The BE is solved analytically through the inverse scattering transform. The analytical solutions for the BE and NLSE are compared with numerically obtained single-soliton solutions for the two equations respectively. The numerical solutions are conducted using a finite difference method (FDM) based on central difference.

Contents

1 Introduction **3**

2 Background Material **5**
2.1 Basic concepts 5
2.1.1 Nonlinear Evolutionary Equations 5
2.1.2 Solitary Waves and Solitons 6
2.1.3 boomeron- and Trappon Solitons 6
2.2 Equations with boomeron- and Trappon Solutions 6
2.2.1 Korteweg-de Vries Equation 6
2.2.2 Boomeron Equation 7
2.2.3 Nonlinear Schödinger Equation 8
2.2.4 Other Equations 9

3 Investigation **10**
3.1 Problem 10
3.2 Model 10
3.3 Analytical Analysis 10
3.3.1 Inverse Scattering Transform 10
3.3.2 Solving the Boomeron Equation 11
3.3.3 Boomeron Equation - the Soltion Solution 14
3.3.4 Nonlinear Schrödinger Equation - the Soliton Solution 15
3.4 Numerical Analysis 17
3.4.1 Boomeron Equation 18
3.4.2 Nonlinear Schrödinger Equation 18
3.5 Results 19
3.5.1 Boomeron Equation 19
3.5.2 Nonlinear Schrödinger Equation 22
3.6 Discussion 23
3.6.1 Analytical Analysis 23
3.6.2 Numerical Analysis 24

4 Summary and Conclusions **26**

Bibliography **28**

A **30**
A.1 Derivation of the Lax Pair Equation 30
A.2 Generalized Polarization Expressions for the Nonlinear Schrödinger Equation 30

A.3 Numerical Expressions for the Boomeron Equation 31
A.4 Numerical Expressions for the Nonlinear Schödinger Equation 32

Chapter 1

Introduction

Differential equations are of great interest in a number of fields. The equations often describe physical phenomena and have an important role in mathematics. The non-linear differential equations are more difficult to study than the linear counterparts. There are few general techniques, meaning that the nonlinear differential equations often need to be studied one at the time. As for some nonlinear differential equations there exists a transformation resulting in an easier way of solving these equations, e.g. the inverse scattering transform (IST).

A solution of special interest is the *soliton* which is a solution to some nonlinear differential equations. The soliton phenomenon was introduced by the naval engineer John Scott Russell in 1834 as a particle like wave with constant shape and speed, which he called the *solitary wave*. Since then the concept of solitons has been a field of research. In 1965 Zabusky and Kruskal coined the expression soliton for the wave solutions which pass each other without losing neither shape nor velocity [10]. Many different equations have been proven to give rise to soliton solutions including the Korteweg-de Vries (KdV) equation and the nonlinear Schrödinger equation (NLSE). The soliton has come to be important in the field of optical fibers and especially in inhomogeneous fiber systems. These special solutions have been identified in various experiments regarding nonlinear fiber optics [20, 18].

For some systems, where these nonlinear differential equations can be used as a model, there exists a direction dependency in which the scalar equations, firstly considered, need to be generalised to coupled nonlinear differential equations. In the application of optical fibers the direction dependency of the soliton solutions can be interpreted as polarization dependency.

In contrast to the scalar nonlinear differential equations, the coupled nonlinear differential equations can give rise to soliton solutions with changing velocity. This property can alter the direction of propagation for the soliton solution. The two special solitons with this property, treated in this report, are the *boomeron*- and the *trappon* solitons. For the boomeron solitons the direction of propagation will only change once, as for the trappon solitons it changes multiple times. After a careful literature survey these interesting solutions have not been found in experimental reports, thus, they are still pure theoretical phenomena.

The boomeron was first discovered in 1976 by F. Calogero and A. Degasperis who after analyzing an equation, which they later named the *Boomeron equation* (BE), found a soliton that after being sent in one direction came back, thus the name boomeron [3].

Calogero and Degasperis also introduced another type of soliton, the trappon soliton. A solution which is trapped in a specific region of space, hence the name trappon soliton. When plotting this single-soliton solution with respect to time it will oscillate in the same region of space indefinitely. The boomeron- and trappon solitons are the two different types of solitons that will be discussed in this report.

This report will begin with an introduction to the basic concepts of the subject and the historical background of the equations. Subsequently, the analytical solution for the BE will be derived through the IST, which is a powerful tool in the field of nonlinear differential equations. An analytical and numerical analysis of the BE and the NLSE will be conducted. The analytical investigation will contain an in-depth investigation of the velocity-polarization relation. Finally the analytical and numerical solutions will be compared.

Chapter 2

Background Material

.

In this chapter a brief introduction to nonlinear evolutionary equations and the soliton solution is given. The characteristics of the boomeron- and trappon solitons are described. This is followed by the background of the Korteweg-de Vries (KdV) equation which has been of great importance historically in the field of solitons, as well as in the specific field of boomerons and trappons. The background of the BE and the NLSE is then described. The chapter ends with a presentation of other equations having boomeron- and trappon solutions.

2.1 Basic concepts

2.1.1 Nonlinear Evolutionary Equations

The equations treated in this text are nonlinear partial differential equations describing the time evolution of a physical field; nonlinear evolutionary equations. The evolutionary equations often depend on several space variables, however, the equations treated in this report are restricted to only one spatial variable. Historically, the linearized versions of these equations have been studied widely due to the complexity of the nonlinearity. Gardner *et al.* made a large contribution to the theory when solving the KdV equation in a new way [13]. This was then generalized by Peter Lax a few years later by introducing the *Lax pair*, which led to further breakthroughs for other equations such as the NLSE [14].

The solutions to these nonlinear evolutionary equations studied in this report are restricted to a group defined by the rate in which they decrease; they vanish exponentially or faster in the spatial dimension. This is a common constraint in the nonlinear evolutionary theory in general and in the case of soliton solutions this does not limit the solutions in any way. The constraint can be described mathematically as [4]

$$\lim_{x\to\pm\infty} e^{\epsilon|x|}u(x) = 0. \tag{2.1}$$

Generalization of Nonlinear Evolutionary Equations

The nonlinear evolutionary equations were first studied in their scalar versions due to their simplicity. However, there are several applications, such as the propagation of light

in a nonlinear fiber with birefringence, that requires a vector equation. This direction dependency can be applied to various equations even though the physical interpretation may be more or less concrete. As mentioned earlier the direction dependency of the NLSE can be viewed as a polarization dependency. For convenience the term polarization will be used throughout this report to describe this direction dependency for all the treated equations. In the case of the boomeron- and trappon soliton solutions a polarization dependent equation is required in order for these special solutions to occur.

2.1.2 Solitary Waves and Solitons

John Scott Russell's discovered 1834 a wave traveling with a constant shape and speed which he called the *Wave of Translation*. This wave was described as a *solitary elevation* which led to the name *solitary wave* for the waves with constant shape and velocity [18]. The solitary wave was further investigated and led to the expression *soliton*, coined by Zabusky and Kruskal in 1965, for the wave solutions which pass each other without changing neither shape nor velocity [10]. Soliton solutions can be divided into multi- and single-soliton solutions. The multi-soliton solution has numerous solitons in its solution, while the single-soliton solution only has one. Solitons can be seen as particle like solutions of nonlinear evolutionary equations. The solitons appear in these equations due to the effects of dispersion and nonlinearity.

If a wave, or more specifically a pulse, propagates in a medium with a dispersive effect the pulse will spread out. On the contrary, if the pulse propagates in a nonlinear medium this can have a narrowing effect. If these two phenomena are combined the effects of broadening and narrowing can cancel and the result is a soliton [18].

2.1.3 boomeron- and Trappon Solitons

Up until 1976 the solitons investigated had constant velocity. The most crucial step towards solitons with changing velocity was taken in 1976 by F. Calogero and A. Degasperis when generalizing the KdV equaiton [9, 4]. F. Calogero and A. Degasperis investigated the simplest version of the generalization and found that the velocity of the solitons was, in general, no longer constant. They coined the expression boomeron for the solitons only changing the direction of propagation once and later also the expression trappon for the solitons trapped oscillating in a spatial domain [3]. In the boomeron- and trappon soliton context the single-soliton solution is of particular interest. The solutions investigated in this report are restricted to these single-soliton solutions.

2.2 Equations with boomeron- and Trappon Solutions

2.2.1 Korteweg-de Vries Equation

Diederik Korteweg and Gustav de Vries derived the following equation in 1895

$$u_t + u_{xxx} - 6uu_x = 0, \tag{2.2}$$

where u_{xxx} describes dispersion and the term uu_x contains a narrowing effect [11, 17]. The equation, called the KdV equation, is a nonlinear partial differential equation and

its soliton solutions can be solved exactly by applying the IST. An introduction to the IST will be presented later in this report in Sec. 3.3.1.

The KdV equation is a mathematical model that describes the theory of water waves in shallow channels. The KdV equation has become of significant importance in the field of solitons due to the fact that it describes an observed natural phenomenon and that its solutions can be exactly determined. There are many different types of the KdV equation, but the one presented in Eq. (2.2) is the most common one. Due to the fact that Eq. (2.2) is a scalar equation it cannot generate neither a boomeron- nor a trappon soliton [9, 8]. Instead a more generalized, modified, KdV equation is required.

Generalization of the KdV Equation

In order to obtain a generalized equation, different polarizations are introduced into Eq. (2.2) by letting $u(x,t)$ be a matrix, $U(x,t)$, and the scalar constants in front of the terms, here named c_0 and c_1, be matrices, C_0 and C_1, [9, 8]. The generalized equation can be written as

$$U_t + i[C_0, U] + \tfrac{1}{2}\{C_1, U_x\} + [W, U] = 0, \quad W_x = \tfrac{1}{2}[C_1, U], \quad W(-\infty, t) = 0, \tag{2.3}$$

where $[C_1, U_x]$ is the commutator $[C_1, U_x] = C_1U_x - U_xC_1$, $\{C_1, U_x\}$ is the anti-commutator $\{C_1, U_x\} = C_1U_x + U_xC_1$ and $W(x,t)$ in an auxiliary field, which is needed as a result of the scalar constants becoming matrices. The soliton solutions of Eq. (2.3) describe, in general, accelerated solitons and can, with suitable choices of the matrices, give rise to boomeron- and trappon solitons. The simplest version of Eq. (2.3), still generating boomeron- and trappon solitons, is the BE [3, 9]. This important equation in the field of boomeron- and trappon theory will be discussed in the next section.

2.2.2 Boomeron Equation

The BE was first introduced by Antonio Degasperis and Fransesco Calogero in [3], presenting the boomeron phenomenon, in 1976. In its original form it reads

$$\begin{aligned} u_t(x,t) &= \boldsymbol{b} \cdot \boldsymbol{v}_x(x,t), \\ \boldsymbol{v}_t(x,t) &= \boldsymbol{b}u_x(x,t) + \boldsymbol{a} \times \boldsymbol{v}(x,t) + \boldsymbol{b}v^2(x,t) - \boldsymbol{v}(x,t)\left[\boldsymbol{b} \cdot \boldsymbol{v}(x,t)\right] + \\ &\quad + \boldsymbol{b} \times \int_x^\infty \boldsymbol{v}(x',t) \times \boldsymbol{v}_x(x',t)dx'. \end{aligned} \tag{2.4}$$

This is a coupled nonlinear evolution equation where $u(x,t)$ is a scalar field, $\boldsymbol{v}(x,t)$ is a three dimensional vector field and $\boldsymbol{a}$ and $\boldsymbol{b}$ are two constant three dimensional vectors. Consequently throughout this report bold letters, e.g. $\boldsymbol{a}$, represent vectors.

The BE is of particular interest in the field of boomeron- and trappon solitons since these phenomena were discovered through this equation. However, it should be pointed out, that the single-soliton solution is contained in the partial derivatives, $u_x(x,t)$ and $\boldsymbol{v}_x(x,t)$. This will be discussed further in Sec. 3.3.2 and Sec. 3.3.3.

The BE, Eq. (2.4), can be rewritten into different forms. By differentiating the second equation in Eq. (2.4) the following form is obtained [6]

$$
\begin{aligned}
u_t(x,t) &= \boldsymbol{b}\cdot\boldsymbol{v}_x(x,t),\\
\boldsymbol{v}_{xt}(x,t) &= \boldsymbol{b}u_{xx}(x,t) + \boldsymbol{a}\times\boldsymbol{v}_x(x,t) - 2\boldsymbol{v}_x(x,t)\times\left[\boldsymbol{v}(x,t)\times\boldsymbol{b}\right].
\end{aligned}
\tag{2.5}
$$

In this form the integral part of the equation is avoided resulting in a pure partial differential equation while the form in which it was first introduced is a integro-differential equation [5].

As for the other equations treated in this report a polarization is needed for the boomeron- and trappon phenomena to emerge. In Eq. (2.4) and Eq. (2.5) this property is contained in the vector field, $\boldsymbol{v}(x,t)$.

2.2.3 Nonlinear Schödinger Equation

The other equation, apart from the BE, investigated in this report is the NLSE. The NLSE has many different types of applications such as the propagation of a laser beam in various media and water waves. The equation is applicable when the nonlinearities are weak but there is a finite dispersion. The name of the equation is due to the close connection to the linear Schrödinger equation. The equation can be written in a number of different ways, one of the most frequently used reads

$$
u_t = i\left(\frac{1}{2}u_{xx} + \kappa|u|^2u\right),
\tag{2.6}
$$

where $u = u(x,t)$ is a complex function and κ is an arbitrary non-zero constant [19].

In the application of light propagation, in various media and especially in fiber optics, the nonlinear term in Eq. (2.6) comes from the change in refractive index when an electrical field is applied to the media, this is called the optical Kerr effect. The electrical field can either be externally applied or produced by the propagating light beam. The Kerr effect produced by the light beam itself is well known as *self-modulation* [10].

The NLSE can be solved by the IST using the Zakharov-Shabat system as the eigenvalue equation resulting in soliton solutions, both single- and multi-soliton solutions [10, 21]. Eq. (2.6) is, however, too simple to give rise to boomeron- and trappon solitons. In order to obtain these kind of solutions Eq. (2.6) must be generalized.

Generalization of the Nonlinear Schödinger Equation

The first step in generalizing the NLSE is to consider the different polarization directions. This was done by S. V. Manakov [15] in which the following coupled equations were obtained

$$
\begin{aligned}
u_t^{(1)} &= i\left(\frac{1}{2}u_{xx}^{(1)} + \kappa(\left|u^{(1)}\right|^2 + \left|u^{(2)}\right|^2)u^{(1)}\right)\\
u_t^{(2)} &= i\left(\frac{1}{2}u_{xx}^{(2)} + \kappa(\left|u^{(1)}\right|^2 + \left|u^{(2)}\right|^2)u^{(2)}\right)
\end{aligned}
\tag{2.7}
$$

where u_1 and u_2 are two components. Eq. (2.6) is recovered by setting one of the two components to zero.

However, the Kerr effect described by Eq. (2.7) is still to simple to give rise to boomeron- and trappon solitons. In order to obtain these solutions the NLSE is generalized to the following system

$$
\begin{aligned}
U_t(x,t) = \left[C^{(0)}, U(x,t)\right] + \sigma\left[C^{(1)}, U_x(x,t)\right] - \sigma\left\{U(x,t), W(x,t)\right\} \\
-i\sigma\left[U_{xx}(x,t) - 2U^3(x,t)\right], \\
W_x(x,t) = \left[C^{(1)}, U^2(x,t)\right],
\end{aligned}
\tag{2.8}
$$

were $U(x,t)$, $C^{(0)}$ and $C^{(1)}$ are matrices, $W(x,t)$ is an auxiliary field, $\left[C^{(0)}, U(x,t)\right]$ and $\{U(x,t), W(x,t)\}$ are the commutator and anti-commutator as for the generalized KdV equation in Eq. (2.3). Eq. (2.8) contains the most generalized type of kerr effect constructed from Eq (2.6), still integrable and solvable by the IST [9].

In order to simplify the analytical solutions and the numerical implementation the simplest version of Eq. (2.8), still generating boomeron- and trappon solutions, will be investigated in this report. This version can be seen as an extension of the Manakov system presented in Eq. (2.7) and is on the form

$$
\begin{aligned}
u_t^{(1)} &= -au^{(2)} + bu_x^{(1)} + wu^{(2)} + i\left[u_{xx}^{(1)} + 2\left(|u^{(1)}|^2 + |u^{(2)}|^2\right)u^{(1)}\right] \\
u_t^{(2)} &= a^*u^{(1)} - bu_x^{(2)} + w^*u^{(1)} + i\left[u_{xx}^{(2)} + 2\left(|u^{(1)}|^2 + |u^{(2)}|^2\right)u^{(2)}\right] \\
w_x &= 2bu^{(1)}u^{(2)*}, \;\; w(-\infty,t) = 0.
\end{aligned}
\tag{2.9}
$$

The system describes quadratic and cubic Kerr-type coupling together with Schrödinger-type dispersion [9].

2.2.4 Other Equations

In this report the BE and the NLSE, previously presented, will be investigated further analytically and numerically due to their importance in the boomeron- and trappon theory. However, other equations have also been found to give rise to the boomeron- and trappon phenomenon. Though not investigated further, these equations are presented below.

Eckhaus Equation

The *2-vector Eckhaus equation* has been found to generate boomeron solutions [7]. The nonlinear coupled differential equation reads

$$
\begin{aligned}
iU_t + AU_{xx} + (U, BU)_x AU + 2(U, BU)AU_x \\
+ \left[(U_x, BAU) - (U, BAU_x)\right]U + (U, BU)^2 AU = 0,
\end{aligned}
\tag{2.10}
$$

where A and B are real, diagonal (2×2) matrices and $U = U(x,t)$ is a two-component-vector.

Cubic-quintic Ginzburg-Landau Equation

The *Cubic-quintic Ginzburg-Landau equation*, also known as the *Newell-Whitehead equation* in the field of fluid mechanics, can give rise to a trappon phenomenon [16]. The equation is on the form

$$
U_t = \epsilon U + (1 + ic_1)U_{xx} + (1 + ic_3)\left|U\right|^2 U - (1 - ic_5)\left|U\right|^4 U, \tag{2.11}
$$

where ϵ, c_1, c_3 and c_5 are real coefficients and $U = U(x,t)$ is a matrix.

Chapter 3

Investigation

The main interest of the investigation is to clarify the velocity-polarization relation. The IST technique and Lax-pair provides the necessary support to conduct an analytical investigation of the boomeron- and trappon single-soliton solutions. The single-soliton solutions are thoroughly described in order to investigate the velocity-polarization relation. Furthermore a numerical investigation will be outlined for the BE and the NLSE. The analytical and numerical solutions to the equations are then compared.

3.1 Problem

The analytical part of this report aims to develop the connection between the velocity and the polarization for the BE. In addition, is there a similar connection for the NLSE? The numerical part will answer the question if it is possible to, in a simple way, simulate the boomeron- and trappon behaviour.

3.2 Model

The investigation consists of a literature survey and an in-depth analysis of the analytical solutions obtained through the IST. These solutions and their polarizations are plotted using MATLAB to illustrate the relation between the changing velocity and the polarization. The solutions to the BE and the NLSE is subsequently compared using the analytical expressions as well as the analytical plots. The numerical part of the model consists of an implementation of these equations using ordinary FDM methods in MATLAB. The solutions of the numerical part are then compared with the analytical solutions.

3.3 Analytical Analysis

3.3.1 Inverse Scattering Transform

The inverse scattering transform was developed by Gardner *et al.* when solving the KdV equation [13]. Peter Lax later generalized this method with the conclusion that the solution involved two linear operators defined on the same complex Hilbert space. The two operators form a Lax pair, which are described further in the following section. After

the generalization by Peter Lax other equations were solved in the same way as the KdV equation including the NLSE and the BE [10].

The IST consists of three parts; the *direct scattering problem*, the *time evolution* of the scattering data and the *inverse scattering problem*, which can be studied in Figure 3.1. For a known potential at a specific time, $q(x, t_0)$, there exists a unique *spectrum* consisting of eigenvalues with corresponding eigenfunctions. Together with the constants for each eigenfunction and the reflection the spectrum form the *scattering data*. Determining this scattering data is known as the direct scatter problem [1, 11]. The next step is finding the time evolution of the eigenfunctions. Finally the potential $q(x, t)$ is constructed through the eigenfunctions and their corresponding time evolution. This is called the inverse scattering problem. The IST is comparable to the Fourier transform.

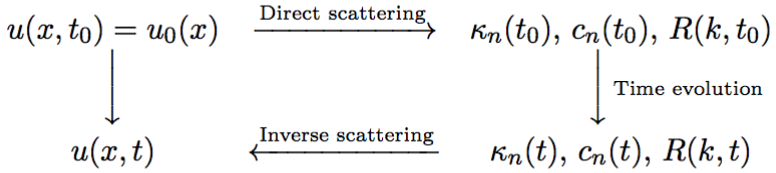

Figure 3.1: Schematic representation of the IST.

Lax Pair

The lax pair terminology of a nonlinear partial differential equation was first introduced by Peter Lax in 1968 and is used in the *Inverse scattering transform* [10, 14]. The Lax pairs are used to solve some nonlinear differential equations by introducing the independent operators L and P, the Lax pairs. The essential property of the Lax pairs is described in the Lax pair equation

$$L_t = PL - LP = [P, L]. \tag{3.1}$$

A derivation of Eq. (3.1) is conducted in Appendix A.1.

The generalizations of the scalar versions of the KdV equation and the NLSE, in Sec. 2.2.1 and Sec. 2.2.3 respectively, are enabled through the Lax pair concept. The generalizations are constructed by replacing scalar variables in the Lax pairs with matrices. This results in the most generalized, and still integrable, equations of KdV and NLSE type [9].

3.3.2 Solving the Boomeron Equation

In this section the BE is solved by the inverse scattering transformation. The following analytical calculation is similar to the calculation found in [3, 6] but slightly rewritten in order to make it easier to understand.

The BE, Eq. (2.5) given in Sec. 2.2.2, is, for convenience, once again presented

$$\begin{aligned} u_t(x,t) &= \boldsymbol{b} \cdot \boldsymbol{v}_x(x,t) \\ \boldsymbol{v}_{xt}(x,t) &= \boldsymbol{b} u_{xx}(x,t) + \boldsymbol{a} \times \boldsymbol{v}_x(x,t) - 2\boldsymbol{v}_x(x,t) \times [\boldsymbol{v}(x,t) \times \boldsymbol{b}]\,. \end{aligned} \tag{3.2}$$

The first step, when solving Eq. (3.2), is to construct the potential $q(x, t_0)$ from the initial conditions for $u_x(x,t)$ and $\boldsymbol{v}_x(x,t)$

$$q(x,t_0) = -u_x(x,t_0) - \boldsymbol{\sigma} \cdot \boldsymbol{v}_x(x,t_0). \tag{3.3}$$

This ansatz is made because, in the case of the BE, it is not $u(x,t)$ or $\boldsymbol{v}(x,t)$ that contains the soliton solution but rather the derivates, $u_x(x,t)$ and $\boldsymbol{v}_x(x,t)$.

The one-dimensional Schrödinger operator, the L-operator in the Lax pair for the BE, is then used to find eigenfunctions with corresponding eigenvalues

$$\left[-\frac{d^2}{dx^2} + q(x,t_0)\right] \psi(x,\lambda,t_0) = \lambda\psi(x,\lambda,t_0), \tag{3.4}$$

where $\psi(x,k,t_0)$ is an eigenfunction and λ is an eigenvalue. The condition stated in Eq. (2.1), Sec. 2.1.1, requiring the potential $q(x,t)$ to decrease exponentially or faster, results in the restriction of $\psi(x,\lambda,t_0)$ beeing a linear combination of $e^{\pm ikx}$ when $x \to \pm\infty$ [12]. This is realized by inserting the condition into Eq. (3.4).

When solving Eq. (3.4), two different solutions are obtained depending on the sign of λ. For $\lambda = k^2 > 0$, were k is a real constant, the solution is on the form

$$\Psi(x,k,t_0) \sim \begin{cases} e^{-ikx} + R(k,t_0)e^{ikx}, & x \to +\infty \\ T(k,t_0)e^{-ikx}, & x \to -\infty. \end{cases} \tag{3.5}$$

$R(k,t_0)$ and $T(k,t_0)$ are the reflection- and transmission coefficient, respectively [3]. These coefficients depend on k. Clearly the following must also be satisfied due to continuity conditions

$$|R(k,t_0)|^2 + |T(k,t_0)|^2 = 1. \tag{3.6}$$

It is evident that through this equation only one of $R(k,t_0)$ and $T(k,t_0)$ is needed to determine $q(x,t)$ and thereby $u_x(x,t)$ and $\boldsymbol{v}_x(x,t)$. In this solution λ, and thereby k, are continuous. Hence this part of the spectrum is called the continuous spectrum [12].

As in the case of $\lambda = -\kappa_n^2 < 0$, there exists a finite set, N, of values κ_n giving rise to solutions on the form

$$\psi_n(x,t_0) \sim \begin{cases} c_n(t_0)e^{-\kappa_n x}, & x \to +\infty \\ \overline{c}_n(t_0)e^{\kappa_n x}, & x \to -\infty. \end{cases} \tag{3.7}$$

These eigenvalues κ_n are discrete values, hence, this part of the spectrum is called the discrete spectrum. In the discrete spectrum the complementary condition becomes [3]

$$\int_{-\infty}^{\infty} (\psi_n(x,t_0), \psi_n(x,t_0))dx = 1. \tag{3.8}$$

As in the case of $R(k,t_0)$ and $T(k,t_0)$ only one of $c_n(t_0)$ and $\overline{c}_n(t_0)$ is needed.

The spectrum of $q(x,t_0)$ consists of both the continues spectrum and the discrete spectrum. An important result is that the function $q(x,t_0)$ has a unique spectrum and, conversely, the spectrum uniquely defines the function $q(x,t_0)$. The scattering data of the potential $q(x,t_0)$ is given by

$$\{\kappa_n(t_0)\}_{n=1}^N, \quad \{c_n(t_0)\}_{n=1}^N, \quad \{R(k,t_0)\}_{k\in\mathbb{R}}. \tag{3.9}$$

Having determined the scattering data the direct scattering problem has now been solved.

The next task at hand is to determine the time evolution of the scattering data expressed in Eq. (3.9). These are obtained through the following relations [3, 12]

$$\begin{aligned} \kappa_n(t) &= \kappa_n(t_0) \\ R(k,t) &= e^{i(t-t_0)\left(-\frac{1}{2}\boldsymbol{a}+k\boldsymbol{b}\right)\cdot\boldsymbol{\sigma}} R(k,t_0) e^{i(t-t_0)\left(\frac{1}{2}\boldsymbol{a}+k\boldsymbol{b}\right)\cdot\boldsymbol{\sigma}} \\ c_n(t)c_n^\dagger(t) &= e^{i(t-t_0)\left(-\frac{1}{2}\boldsymbol{a}+\kappa_n\boldsymbol{b}\right)\cdot\boldsymbol{\sigma}} c_n(t_0)c_n^\dagger(t_0) e^{i(t-t_0)\left(\frac{1}{2}\boldsymbol{a}+\kappa_n\boldsymbol{b}\right)\cdot\boldsymbol{\sigma}}. \end{aligned} \tag{3.10}$$

The final step in the inverse scattering transform is to solve the inverse scattering problem. Through the time evolution of the scattering data, Eq. (3.10), the Marchenko equation is constructed

$$K(x,z,t) + F(x+z,t) + \int_x^\infty K(x,y,t)F(y+z,t)dy = 0, \tag{3.11}$$

where F(x, t) is defined as

$$F(x,t) = \sum_{n=1}^{N} e^{\kappa_n x} c_n(t)c_n^\dagger(t) + \frac{1}{2\pi}\int_{-\infty}^{\infty} e^{ikx} R(k,t)dk. \tag{3.12}$$

The Marchenko equation, Eq. (3.11), has the form of a Fredholm integral equation and can be solved by standard methods [12]. When solved for $K(x,z,t)$, under the condition $K(x,\infty,t) = 0$, $q(x,t)$ is obtained by

$$q(x,t) = -2\frac{\partial}{\partial x}K(x,x,t). \tag{3.13}$$

Through Eq. (3.3) $u(x,t)$ and $\boldsymbol{v}(x,t)$ is determined by

$$u(x,t) + \boldsymbol{\sigma}\cdot\boldsymbol{v}(x,t) = 2K(x,x,t). \tag{3.14}$$

The solution has two different parts, one associated with the the continuous spectrum, $\lambda = k^2 > 0$ and the other with the discrete spectrum, $\lambda = -\kappa_n^2 > 0$. The continuous part can be interpreted as scattering states of the linear Schrödinger operator in Eq. (3.4), as for the descrete part, it can be interpreted as bound states of the same operator.

The soliton part of the solution, consisting of the discrete spectrum, can give rise to boomeron- and trappon solutions and is obtained when the reflection coefficient $R(x,t_0) = 0$, through Eq. (3.10) this clearly implies that $R(x,t) = 0$ [12]. Two potentials having the property of $R(x,t) = 0$ is

$$q_1(x,t) = \frac{C}{\cosh(x-\xi(t))}, \;\; q_2(x,t) = \frac{C}{\cosh^2(x-\xi(t))}, \tag{3.15}$$

C being a constant.

An analytical derivation of the solution for the BE has now been conducted. It should be emphasized for the reader that the boomeron- and trappon single-soliton solution decends from $q(x,t)$, originating from Eq. (3.3).

3.3.3 Boomeron Equation - the Soltion Solution

The analytical solution of the BE obtained from the calculations in the previous section is

$$u(x,t) = -p\frac{e^{-p(x-\xi(t))}}{\cosh[p(x-\xi(t))]}, \;\; \boldsymbol{v}(x,t) = u(x,t)\hat{\boldsymbol{n}}, \tag{3.16}$$

$$\xi(t) = \xi_0 + \frac{1}{2p}\ln\Big[S(t)\Big], \tag{3.17}$$

$$\hat{\boldsymbol{n}}(t) = \frac{\boldsymbol{S}(t)}{S(t)} \tag{3.18}$$

$$\boldsymbol{S}(t) = \boldsymbol{n}_+ e^{a\nu_-(t-t_0)} + \boldsymbol{n}_- e^{-a\nu_-(t-t_0)} + \boldsymbol{s}\sin[a\nu_+(t-t_0)] + \boldsymbol{c}\cos[a\nu_+(t-t_0)], \tag{3.19}$$

$$S(t) = n_+ e^{a\nu_-(t-t_0)} + n_- e^{-a\nu_-(t-t_0)} + \overline{s}\sin[a\nu_+(t-t_0)] + \overline{c}\cos[a\nu_+(t-t_0)], \tag{3.20}$$

$$\begin{aligned}\boldsymbol{n}_\pm = \Big\{&(\nu_+^2-1)\hat{\boldsymbol{n}}_0 + [(\hat{\boldsymbol{a}}\cdot\hat{\boldsymbol{n}}_0) \mp \eta\nu_+]\,\hat{\boldsymbol{a}} + \lambda\left[\lambda(\hat{\boldsymbol{b}}\cdot\hat{\boldsymbol{n}}_0) \mp \nu_-\right]\hat{\boldsymbol{b}} \\ &\pm\nu_-(\hat{\boldsymbol{a}}\times\hat{\boldsymbol{n}}_0) \mp \eta\lambda\nu_+(\hat{\boldsymbol{b}}\cdot\hat{\boldsymbol{n}}_0) - \lambda(\hat{\boldsymbol{a}}\times\hat{\boldsymbol{b}})\Big\}/\nu,\end{aligned} \tag{3.21}$$

$$n_\pm = \frac{1+\nu_-^2 \mp \eta\nu_+(\hat{\boldsymbol{a}}\cdot\hat{\boldsymbol{n}}_0) \mp \lambda\nu_-(\hat{\boldsymbol{b}}\cdot\hat{\boldsymbol{n}}_0) + \lambda\Big((\hat{\boldsymbol{a}}\times\hat{\boldsymbol{b}})\cdot\hat{\boldsymbol{n}}_0\Big)}{\nu} \tag{3.22}$$

$$\nu_\pm = \left\{\left[\lambda^2(\boldsymbol{a}\cdot\boldsymbol{b})^2 + \frac{1}{4}(1-\lambda^2)^2\right]^{1/2} \pm \frac{1}{2}(1-\lambda^2)\right\}^{1/2}, \;\; \nu = 2(\nu_+^2+\nu_-^2), \tag{3.23}$$

$$\boldsymbol{s} = 2\,\frac{\eta\nu_-\hat{\boldsymbol{a}} - \lambda\nu_+\hat{\boldsymbol{b}} + \nu_+(\hat{\boldsymbol{a}}\times\hat{\boldsymbol{n}}_0) + \eta\lambda\nu_-(\hat{\boldsymbol{b}}\times\hat{\boldsymbol{n}}_0)}{\nu}, \tag{3.24}$$

$$\overline{s} = 2\,\frac{\eta\nu_-(\hat{\boldsymbol{a}}\cdot\hat{\boldsymbol{n}}_0) - \lambda\nu_+(\hat{\boldsymbol{b}}\cdot\hat{\boldsymbol{n}}_0))}{\nu}, \tag{3.25}$$

$$\boldsymbol{c} = \hat{\boldsymbol{n_0}} - \boldsymbol{n_+} - \boldsymbol{n_-}, \quad \overline{c} = 1 - n_+ - n_-, \tag{3.26}$$

$$\lambda = \frac{2pb}{a}, \qquad \eta = sign(\hat{\boldsymbol{a}}, \cdot\hat{\boldsymbol{b}}) \tag{3.27}$$

where p and ξ_0 are two arbitrary *real* constants and $\hat{\boldsymbol{n}}_{\boldsymbol{0}}$ is an arbitrary *real* vector. The two most important parts in this solution, in aspect of the boomeron- and trappon behaviour, are $\xi(t)$ and $\hat{\boldsymbol{n}}(t)$ given in Eq. (3.17) and Eq. (3.18) respectively.

Eq. (3.17) describes the position, $\xi(t)$, of the single-soltion solution. Thus the boomeron- and trappon phenomena orignitates from the nonlinearity in Eq. (3.17), in other words when $\xi_{tt} \neq 0$. This nonlinearity is contained in the introduced variable $S(t)$, Eq. (3.20),

being the norm of $\boldsymbol{S}(t)$, in Eq. (3.19), which, in turn, is introduced to describe the three dimensional polarisation field, $\hat{\boldsymbol{n}}(t)$, Eq. (3.18). Thus the nonlinearity in the position of the single-soltion solution originates from the polarisation of the soliton. This will be further investigated in the following section.

The vectors, $\boldsymbol{n}_{\pm}$, in Eq. (3.21) will, in this report, be called the *assymptotic polarizations* due to the behaviour of the solution's polarization. Eq. (3.22) describe the scalar versions of $\boldsymbol{n}_{\pm}$. The constants, $\nu_{\pm}$, in Eq. (3.23) simplify the expressions

By the definition of $q(x,t)$, given in Eq. (3.3), and by studying the solution of $\boldsymbol{v}(x,t)$ in Eq. (3.16), it should be clear that $q(x,t) \propto -u_x(x,t)$. The single-soliton solution, $u_x(x,t)$, has the following analytical expression

$$u_x(x,t) = p^2 \frac{1}{\cosh^2[p(x-\xi(t))]}. \tag{3.28}$$

Eq. (3.28) will be used later in the numerical analysis of the BE, sec. 3.4.1, and will also be plotted in sec. 3.5.

Investigation of the Polarisation

As mentioned above, the boomeron- and trappon behaviour originates from the polarization vector, $\hat{\boldsymbol{n}}(t)$. By studying Eq. (3.19) and Eq. (3.20) it is clear that, in general, the exponential terms, $e^{\pm a\nu_-(t-t_0)}$, will be dominant for $t \to \pm\infty$. Thus $\hat{\boldsymbol{n}}(t) \to \hat{\boldsymbol{n}}_-$ for $t \to -\infty$ and $\hat{\boldsymbol{n}}(t) \to \hat{\boldsymbol{n}}_+$ for $t \to \infty$. Through the connection, $S(t)$, between the polarization vector, $\hat{\boldsymbol{n}}(t)$, and the position, $\xi(t)$, the boomeron behaviour can be explained. The change in polarizarization will result in the solution coming asymptotically from one side, subsequently turning, moving asymptotically in the opposite direction. However, in the intermediate region the sinusoidal terms can play a significant role, making the boomeron follow different trajectories before asymptotically tending towards $\hat{\boldsymbol{n}}_+$.

For the special case when $(\boldsymbol{a}\cdot\boldsymbol{b}) = 0$, the variable $\nu_- = 0$, in Eq. (3.19) and Eq. (3.20). This will make the exponential terms constants, limiting the time dependency to the sin and cos terms. If $n_- + n_+ > \sqrt{\bar{s}^2 + \bar{c}^2}$ the polarization will follow a periodical trajectory and hence the position, $\xi(t)$, of the single-soliton solution will oscillate indefinitely, being a trappon. It is worth mentioning that if $n_- + n_+ \gg \sqrt{\bar{s}^2 + \bar{c}^2}$ the oscillation will be close to insignificant. However, if $n_- + n_+ \leq \sqrt{\bar{s}^2 + \bar{c}^2}$, a part or a point of the polarization will be forbidden due to the logarithmic term for the position, $\xi(t)$ in Eq. (3.19). For some t along the trajectory a singularity will emerge, since $\log(x \leq 0)$ is undefined. Hence, instead of a oscillating, the single-soliton solution will come asymptotically from one side, decelerating, then subsequently moving asymptotically in the opposite direction, being a boomeron.

3.3.4 Nonlinear Schrödinger Equation - the Soliton Solution

The nonlinear coupled Schrödinger equation investigated in this report, derived in Sec. 2.2.3, is, for convenience, presented once again

$$
\begin{aligned}
u_t^{(1)} &= -au^{(2)} + bu_x^{(1)} + wu^{(2)} + i\left[u_{xx}^{(1)} + 2\left(|u^{(1)}|^2 + |u^{(2)}|^2\right)u^{(1)}\right] \\
u_t^{(2)} &= a^* u^{(1)} - bu_x^{(2)} + w^* u^{(1)} + i\left[u_{xx}^{(2)} + 2\left(|u^{(1)}|^2 + |u^{(2)}|^2\right)u^{(2)}\right] \\
w_x &= 2bu^{(1)}u^{(2)*}, \;\; w(-\infty, t) = 0.
\end{aligned} \tag{3.29}
$$

If the IST is applied to Eq. (3.29) in the same way as described for the Boomeron equaiton in Sec. 3.3.2, a single-soliton solution is obtained. The calculations, using the IST, will not be performed for the NLSE in this report due to the great similarities with the calculations performed in Sec. 3.3.2. The single-soliton solution is given by

$$
\begin{pmatrix} u^{(1)} \\ u^{(2)} \end{pmatrix} = \frac{pe^{-ikx}}{\cosh\left[p(x-\xi(t))\right]} \begin{pmatrix} A^{(1)}(t) \\ A^{(2)}(t) \end{pmatrix} \tag{3.30}
$$

$$
\xi(t) = \xi_0 - 2kt + \frac{1}{2p}\log\left[\frac{S(0)}{S(t)}\right], \tag{3.31}
$$

$$
S(t) = 4\,|a|^2\,|\sinh[\alpha t + \mu]|^2 + 4\,|(\alpha\cosh[\alpha t + \mu] - b(p - ik)\sinh[\alpha t + \mu]|^2, \tag{3.32}
$$

$$
\begin{aligned}
A^{(1)}(t) &= -2a \cdot [(S(t)]^{-1/2}\sinh[\alpha t + \mu]e^{i(p^2-k^2)t}, \\
A^{(2)}(t) &= 2 \cdot [S(t)]^{-1/2}\left(\alpha\cosh[\alpha t + \mu] - b(p - ik)\sinh[\alpha t + \mu]\right)e^{i(p^2-k^2)t}
\end{aligned} \tag{3.33}
$$

$$
\alpha = \left[b^2(p - ik)^2 - |a|^2\right]^{1/2}, \tag{3.34}
$$

$$
w(x,t) = 2bp\left(1 + tanh\left\{p[x - xi(t)]\right\}\right)A^{(1)}\left(A^{(2)}\right)^*, \tag{3.35}
$$

where p, k and ξ_0 are three arbitrary *real* constants and μ is an arbitrary complex constant [2].

As for the BE, the variable $\xi(t)$, Eq. (3.31), describes the position of the single-soliton solution and, hence, the nonlinear velocity that is significant for the boomeron- and trappon solitons. The nonlinear part of the position, $\xi(t)$, is contained in the last term in the parameter $S(t)$, described in Eq. (3.32). $A^{(1)}(t)$ and $A^{(2)}(t)$, Eq. (3.33), characterize the two polarization $u^{(1)}(x,t)$ and $u^{(2)}(x,t)$, respectively and therefore have the property

$$
\left|A^{(1)}(t)\right|^2 + \left|A^{(2)}(t)\right|^2 = 1. \tag{3.36}
$$

This property is due to the parameter $S(t)$, here working as a normalization for $A^{(1)}(t)$ and $A^{(2)}(t)$. The parameter α is of great help when determining the properties of the solution, by introducing α the behaviour of the solution can be determined by appropriate choices of the input parameters a, b, p and k. Eq. (3.35) describes the solution for auxiliary field $w(x,t)$.

The single-soliton solution, Eq. (3.30) to Eq. (3.34), exhibits trappon behaviour when α is purely imaginary, this happens when $k = 0$ and

$$
b^2p^2 - |a|^2 < 0. \tag{3.37}
$$

In this case the soliton is trapped in a domain in space. Otherwise the soliton behaves as a boomeron in the reference frame moving with the velocity $-2k$, se Eq. (3.31). The

soliton then comes from one side subsequently decelerates and returns from where it came. During the time evolution the single-solitons exhibit constant shape. For the asymptotic behaviour the soliton moves uniformly with almost constant velocity. In between the asymptotic behaviour for $t = \pm\infty$ the soliton may have several different trajectories depending on the parameters of the equation, a and b, and the constants p, k and μ [2].

Investigation of the Polarization

In order to further understand the relationship between the polarization and the changing velocity for the boomeron- and trappon solitons respectively, $A^{(1)}(t)$ and $A^{(2)}(t)$ can be investigated. In order to apply the polarization analogy to the single-soliton solution of the NLSE, $A^{(1)}(t)$ and $A^{(2)}(t)$ are interpreted as orthogonal polarizations. The investigation outlined in this section regards solutions for $k = 0$. This is a necessary condition for the trappon solitons and in the case of the boomeron solitons this only changes the frame of reference. For the most generalized expression with $k \neq 0$ see Appendix A.2.

In the case of the boomeron solitons, with $k = 0$, α becomes a real constant determined by Eq. (3.34). Since $\sinh[\alpha t+\mu]$ and $\cosh[\alpha t+\mu]$ then becomes strictly increasing functions for $t > 0$, $\left|A^{(1)}(t)\right|^2$ will start at a relatively low value and increases to a maximum due to the normalization of $S(t)$. On the other hand $\left|A^{(2)}(t)\right|^2$ starts at a higher value and subsequently decreases with time. This time evolution of the polarization for the NLSE is directly comparable with the equivalent time evolution described for the BE.

As for the trappon solution, with $k = 0$ and α purely imaginary the polarizations can be rewritten to

$$\begin{aligned} A^{(1)}(t) &= -2a \cdot [(S(t)]^{-1/2} \sin[\beta t + \varphi] e^{i(p^2-k^2)t}, \\ A^{(2)}(t) &= 2 \cdot [S(t)]^{-1/2} \left(\beta \cos[\beta t + \varphi] - b(p - ik) \sin[\beta t + \varphi]\right) e^{i(p^2-k^2)t} \end{aligned} \tag{3.38}$$

where $i\beta = \alpha$ and $i\varphi = \mu$. This expression accentuate the oscillating behaviour of the polarizations in the case of the trappon solitons. The polarizations, will oscillate with the same frequency, depending on β.

3.4 Numerical Analysis

In this section the numerical analysis of this report are outlined. The BE and the NSLE are treated numerically by a finite difference method (FDM) using central difference and plotted in MATLAB. There are two reasons for the choice of central difference instead of the more stable backward Euler. Firstly, an interesting aspect is if this phenomenon can be generated from this more simple numerical model. The second reason for choosing central difference instead of backward Euler is the drawback of the high complexity arising in the backward Euler method, since for each time step a nonlinear equation need to be solved numerically.

The FDM is implemented as approximation of the derivations in the spatial and temporal dimensions. This is done by introducing the discrete set of points $\{x_i\}_{i=1}^n$ and $\{t_j\}_{j=1}^m$ instead of the continuous variables x and t. The difference between successive discrete points in each set are constant, i.e.

$$\Delta x_i = x_i - x_{i-1} = h, \;\; \Delta t_j = t_j - t_{j-1} = t_s. \tag{3.39}$$

Thus the following approximations of the first derivative are obtained using central difference

$$u_x(x_i, t_j) = \frac{u_{i+1,j} - u_{i-1,j}}{2h}, \tag{3.40}$$

$$u_t(x_i, t_j) = \frac{u_{i,j+1} - u_{i,j-1}}{2t_s}, \tag{3.41}$$

where $u_{i,j}$ represent $u(x_i, t_j)$. For the numerical calculations for the NLSE the second spatial derivative in space is also needed,

$$u_{xx}(x_i, t_j) = \frac{u_{i+1,j} + u_{i-1,j} - 2u_{i,j}}{h^2}. \tag{3.42}$$

After substitute these approximations into Eq. (2.9) and Eq. (2.5), an approximation of the time evolution of the equations can be determined. This is done in the two following sections, for each equation respectively.

However, in order to solve this system numerically, an initial value $u_{i,1}$ is needed. This value is established by using the results obtained from the analytical section for each equation, thus setting $t = 0$.

3.4.1 Boomeron Equation

As mentioned earlier, the boomeron- and trappon behaviour is contained in $u_x(x, t)$. To get an explicit expression for $u_x(x, t)$ directly, when applying the FDM, a derivative in space is conducted on the $u_t(x, t)$ expressed in Eq. (2.5). Instead of getting an explicit expression of $\boldsymbol{v}(x, t)$ when applying the FDM approximation, an explicit expression for $\boldsymbol{v}_x(x, t)$ is more suitable for the task at hand. This however, implies an introduction of an auxiliary field $\boldsymbol{w}_x(x, t) = \boldsymbol{v}_{\boldsymbol{x}}(x, t) \times \boldsymbol{b}$ to be used in the numerical calculations. After these modifications introduced above, Eq. (2.5) becomes

$$\begin{aligned} u_{xt}(x, t) &= \boldsymbol{b} \cdot \boldsymbol{v}_{xx}(x, t), \\ \boldsymbol{v}_{xt}(x, t) &= \boldsymbol{b} u_{xx}(x, t) + \boldsymbol{a} \times \boldsymbol{v}_x(x, t) - 2\boldsymbol{v}_x(x, t) \times \boldsymbol{w}(x, t), \\ \boldsymbol{w}_x(x, t) &= \boldsymbol{v}_x(x, t) \times \boldsymbol{b}. \end{aligned} \tag{3.43}$$

To calculate the vector $\mathbf{v}_x(x, t)$ numerically each component $v_x^{(1)}$, $v_x^{(2)}$ and $v_x^{(3)}$ are computed separately. The same method is executed when calculating the auxiliary vector field $\boldsymbol{w}_x(x, t)$. For the explicit numerical expressions see Appendix A.3. The plots obtained with this numerical solution are presented in Sec. 3.5 and will be compared with the analytical single-soliton soltions for the BE in Sec. 3.6.2.

3.4.2 Nonlinear Schrödinger Equation

For the NLSE, Eq. (3.29), the theory behind the numerical analysis is analogous to the one presented for the BE in the previous section. As for the BE, the explicit expressions for the FDM approximations are found in Appendix A.4. The boundary condition, $w(-\infty, t) = 0$ is applied by setting $w(x_1, t_j) = 0$, where x_1 is the lowest value in the

discrete spatial set. In order to avoid divergence the *Dirichlet boundary condition* is also used, setting the boundaries, $u^{(1)}(x_1, t_j)$, $u^{(2)}(x_1, t_j)$ and $u^{(1)}(x_n, t_j)$, $u^{(2)}(x_n, t_j)$ to zero. This decisive step is made after comparing the analytical solutions close to the boundaries, hence validating the use of the Dirichlet boundary conditions presented above.

To initialize the numerical calculations, the single-soltion solutions obtained from the analytical calculations, Eq. (3.30), are used. The plots for the numerical analysis for the NLSE can be studied in Sec. 3.5 together with the analytical solutions for comparison.

3.5 Results

In this section the plots of the analytical and numerical solutions to the BE and the NLSE are presented. The plots consists of both the single-soliton solutions and polarization plots for the corresponding solutions. The plots are produced using the same spacial and temporal steps in order to improve the comparison between the analytical and numerical single-soliton solutions.

3.5.1 Boomeron Equation

The following plots were obtained for the BE. Figure 3.2 presents the numerical and analytical solutions for a set of parameters resulting in a boomeron solution for the numerical solution but only the asymptotic behaviour for the analytical solution.

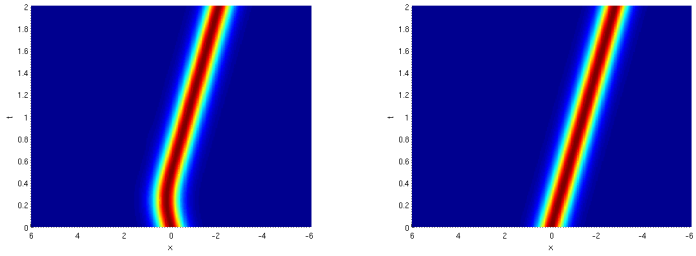

(a) Numerical simulation (b) Analytical simulation

Figure 3.2: Numerical- and analytical solution simulated with $h = 0.05$, $ts = 0.000025$, $\boldsymbol{a}$ = [1 1 0], $\boldsymbol{b}$ = [1 -1 0], $\hat{\boldsymbol{n}}_0$ = [-3 1 0], $p = 2$, $\xi_0 = 0$ and $\lambda = 4$

In Figure 3.3, conversely, the numerical solution shows no change of the direction of propagation while the analytical solution exhibits boomeron behaviour.

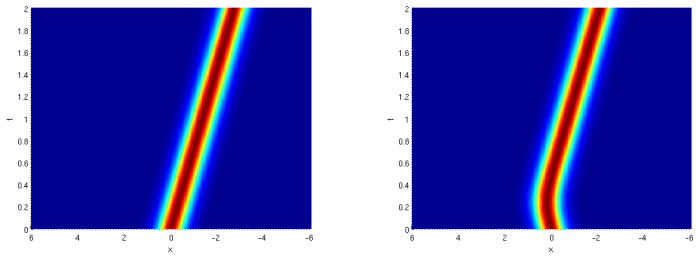

(a) Numerical simulation (b) Analytical simulation

Figure 3.3: Numerical- and analytical solution simulated with $h = 0.05$, $ts = 0.000025$, $\boldsymbol{a}$ = [1 1 0], $\boldsymbol{b}$ = -[1 -1 0], $\hat{\boldsymbol{n}}_0$ = [-3 1 0], $p = 2$, $\xi_0 = 0$ and $\lambda = 4$

In Figure 3.4 both the numerical and analytical solutions exhibit trappon behaviour, but a slight difference is noticed, most noticeable for $t = 0$ and $t = 4$.

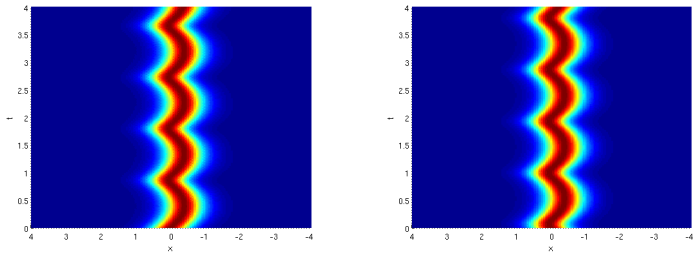

(a) Numerical simulation (b) Analytical simulation

Figure 3.4: Numerical- and analytical solution simulated with the parameters h =0.05, $ts = 0.000025$, $\boldsymbol{a}$ = 5 [2.1 0.8 0], $\boldsymbol{b}$ = [-0.8 2.1 0], $\hat{\boldsymbol{n}}_0$ = [-3 1 0], $p = 2$, $\xi_0 = 0$ and λ = 0.8000

The time evolution of the polarization for the analytical solution to the BE is plotted for two different sets of parameters, one when the single-soliton solution exhibits boomeron behaviour, Figure 3.5, and the other when the single-soliton solution exhibits trappon behaviour, Figure 3.6.

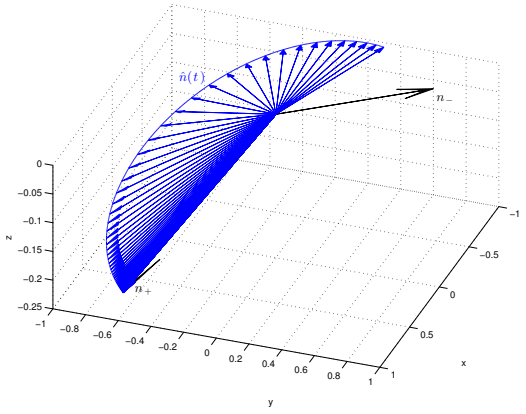

Figure 3.5: Plot of the time evolution of the polarization for the analytical boomeron simulated in Fig 3.3b, together with the two asymptotic polarizations n_+ and n_- (black)

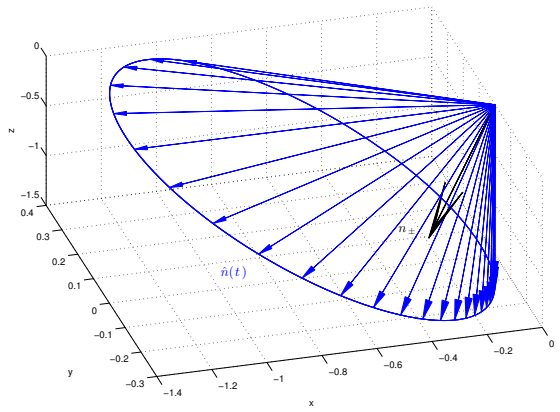

Figure 3.6: Plot of the time evolution for the polarization for the analytical trappon simulated in Fig 3.4b, together with the two asymptotic polarizations n_+ and n_-

In Figure 3.7 the polarization trajectories for the analytical- and numerical solutions described by the same set of parameters, resulting in a boomeron behaviour for the analytical solution and only the asymptotic behaviour for the numerical solution, is displayed in the same plot using two different angles. The corresponding single-soliton solutions for these parameters are displayed in Figure 3.3.

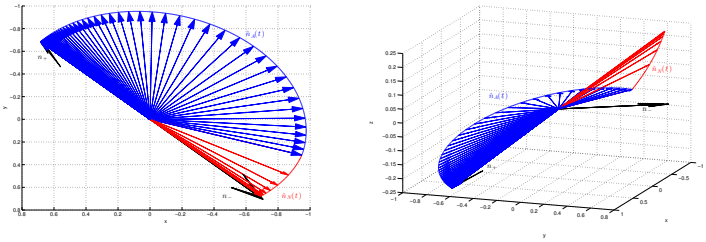

(a) Seen from above (b) Seen from the side

Figure 3.7: Plot of the time evolution of the polarization, from two different angles, for the analytical boomeron, $\hat{\boldsymbol{n}}_A(t)$ (blue), and numerical boomeron, $\hat{\boldsymbol{n}}_N(t)$ (red), simulated in Fig 3.3, together with the two asymptotical polarizations n_+ and n_-

The last two figures, presented in Figure 3.8, show the polarization trayectories for the numerical- and analytical trappon showed in Figure 3.4.

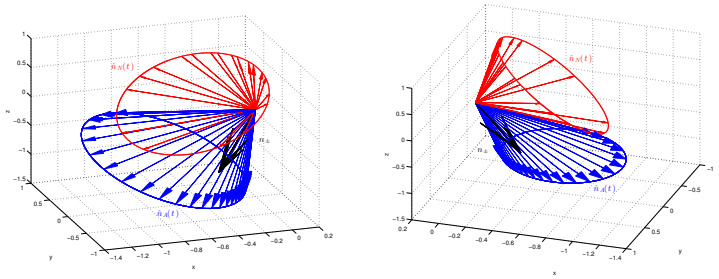

(a) Seen from above (b) Seen from the side

Figure 3.8: Plot of the time evolution of the polarization, from two different angles, for the analytical trappon, $\hat{\boldsymbol{n}}_A(t)$ (blue), and numerical trappon, $\hat{\boldsymbol{n}}_N(t)$ (red), simulated in Fig 3.3, together with the two asymptotical polarizations n_+ and n_-

3.5.2 Nonlinear Schrödinger Equation

For the NLSE simulation, firstly, a comparison for the boomeron- and trappon solutions are presented in Figure 3.9 and Figure 3.10.

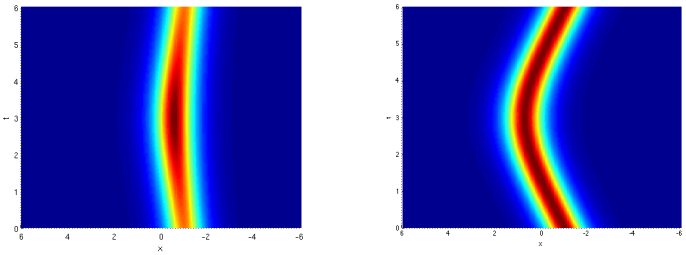

(a) Numerical (b) Analytical

Figure 3.9: Numerical- and analytical solution with the parameters $h = 0.05$, $ts = 0.000025$, $a = 0.01$, $b = 0.2$, $p = 2$, $k = 0$, $\xi_0 = -1$ and $\mu = 1$

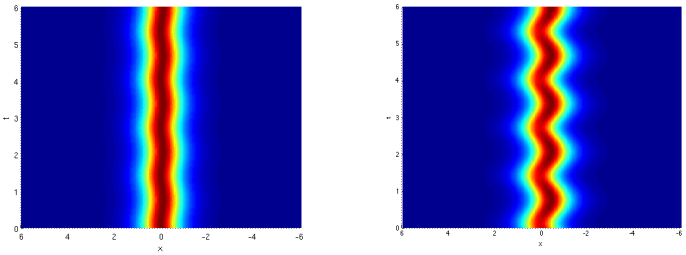

(a) Numerical (b) Analytical

Figure 3.10: Numerical- and analytical solution with the parameters $h = 0.05$, $ts = 0.000025$, $a = 4.5$, $b = 1.9$, $p = 2$, $k = 0$, $\xi_0 = 0$ and $\mu = 1$

Secondly, in order to give a better understanding of the polarization dependency, plots of the analytical polarizations $u^{(1)}$ and $u^{(2)}$ is presented in Figure 3.11 for the boomeron in Figure 3.9b.

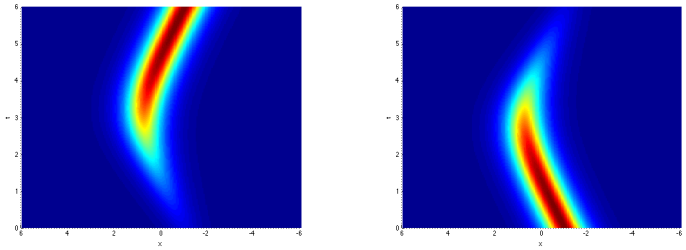

(a) Analytical $u^{(1)}$ (b) Analytical $u^{(2)}$

Figure 3.11: Plots of the analytical polarizations $u^{(1)}$ and $u^{(2)}$with the parameters $h = 0.1$, $ts = 0.00005$, $a = 0.01$, $b = 0.2$, $p = 2$, $k = 0$, $\xi_0 = -1$ and $\mu = 1$

Furthermore, the two polarizations are plotted in Figure 3.12 for the analytical trappon single-soliton solution presented in Figure 3.10b.

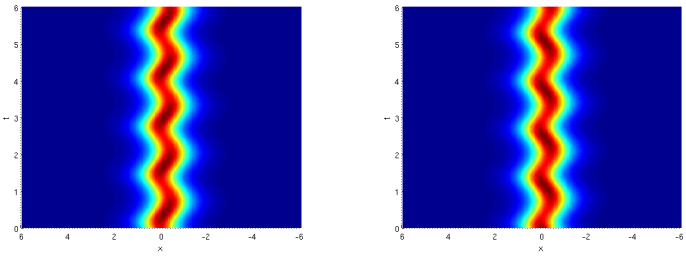

(a) Analytical $u^{(1)}$ (b) Analytical $u^{(2)}$

Figure 3.12: Plots of the analytical polarizations $u^{(1)}$ and $u^{(2)}$with the parameters $h = 0.05$, $ts = 0.000025$, $a = 4.5$, $b = 1.9$, $p = 2$, $k = 0$, $\xi_0 = 0$ and $\mu = 1$

3.6 Discussion

3.6.1 Analytical Analysis

The analytical solutions for the BE and the NLSE, outlined in Sec. 3.3.3 and Sec. 3.3.4, clearly describes the connection between the the changing velocity and the polarization for the two different equaitons. The presentation of this connection, in the case of the BE, is more detailed then the one given in [3]. To make the connection between the polarization and the changing velocity clearer the variable $S(t)$, Eq. (3.20), is introduced. A corresponding variable $S(t)$, Eq. (3.32), is used for the NLSE. This introduction makes the polarization-velocity connection clear and the need of coupled equations obvious.

For the NLSE the vector notation is not used neither in the equation nor in the solution. In order to compare the solution for the BE with the solution for the NLSE a physical interpretation of the two components in the NLSE solution is needed. The two components, $u^{(1)}$ and $u^{(2)}$, are interpreted as orthogonal polarizations specified by the component specific parameters $A(1)$ and $A(2)$. This interpretation makes it possible to investigate if the change in polarization for the NLSE solution has the same properties as the solution of the BE.

The main difference between the two solutions is that the polarization of the BE take place in three dimensions in space while the polarization for the NLSE is bound

to two dimensions in space. The three dimensional trajectory for the polarization of the Boomeoron equation described in Sec. 3.3.3 is quite complex. The corresponding trajectories for the NLSE solution, described in Sec. 3.3.4, are much more simple but exhibit similar behaviour.

For the boomeron solitons both polarizations, for the BE and the NLSE, starts almost parallel to one of the asymptotic polarizations having close to a constant velocity. This can be observed in Figure 3.5 and Figure 3.11 for the BE and the NLSE respectively. The asymptotic behaviour when $t \to \infty$ is also very similar for the two equations, in both solutions the polarization approaches the other asymptotic polarization. Neither one of the solutions coincide completely with the unit polarizations. Between the asymptotic polarizations the two solutions exhibit similar behaviour due to the fact that both solutions have sinusoidal terms that can be of significant importance for these times.

The polarizations of trappon solitons for the BE and the NLSE also exhibit similar behaviour. In both cases the introduced variable $S(t)$ contain only a time dependence in the sinusoidal terms. Thus, both polarizations will exhibit a periodic behaviour which can be seen in Figure 3.6 and Figure 3.12.

3.6.2 Numerical Analysis

The numerical analysis for the BE was unsuccessful. Several different programs have been written for the different cases of the equation, i.e. the general case without any conditions for the vectors $\boldsymbol{a}$ and $\boldsymbol{b}$ and the special cases $(\boldsymbol{a} \cdot \boldsymbol{b}) = 0$ and $\boldsymbol{a} \parallel \boldsymbol{b}$.

Figure 3.2 and Figure 3.4 shows that the boomeron- and trappon phenomena is found for the numerical solutions. The boomeron behaviour for the numerical solution, however, is obtained for different values then for the analytical solutions. This is further investigated by displaying the numerical solutions for a set of parameters generating a boomeron solution for the analytical solution in Figure 3.3.

In order to investigate the error in the numerical solution the introduced tool of displaying the trajectory for the polarization during the time evolution is used. This is due to the close connection between the changing velocity and the polarization. In Figure 3.7, displaying the trajectories of the two polarizations, further information regarding the differences between the analytical- and numerical solutions in Figure 3.3 is obtained. The polarization for the analytical solution, Figure 3.7, clearly shows that the polarization moves towards the asymptotic polarization $\boldsymbol{n}_+$ as it should. The numerical solution, on the other hand, moves towards the negative asymptotic polarization $-\boldsymbol{n}_+$. This error analysis implies that one error is the time evolution for the polarization. The determination of the polarization lies in the cross products in the BE. It is therefore likely that the error has occurred in the calculation of the cross products. The calculations have been checked several times in the programs without finding the error.

For the trappon solution displayed in Figure 3.4 the similarities between the analytical- and the numerical solutions are greater. There are, however, differences especially for the times $t = 0$ and $t = 4$, emphasised in Sec. 3.5. The polarization for the analytical- and the numerical solutions are displayed in Figure 3.8. The plots show a large difference in the trajectories of the polarizations which explaine the differences in the single-soliton trappon solutions. The large difference shows that two single-soliton solutions can resemble in the scalar appearance demonstrated by the single-soliton solutions and, simultaniously, have very different polarization trajectories.

By studying Figure 3.9 and Figure 3.10 a significant difference between the numerical- and analytical simulations are observed. One reason is probably the number of FDM approximations needed when solving the NLSE numerically, which decreases the convergence. Furthermore, the errors are even greater when approximating the second spatial derivative in the NLSE, Eq. (3.29). Another possible reason for the loss of accuracy is that some of the terms in Eq. (3.29), are of power three, resulting in errors rapidly multiplying throughout the solution. In addition, if $u^{(1)}$ or $u^{(2)}$ is small, these nonlinear terms will become even smaller, hence the possibility of round-off errors is substantial.

In order to improve convergence, smaller values of the discretization in time and space, i.e h and t_s, was made for the BE and the NLSE but the convergences did in fact decrease instead of improving. This was probably due to round-off errors occurring when the discretization values were too small. In other words, there exists optimal values for h and t_s in order to give the best convergence.

By comparing the two numerical solutions, for the BE and for the NLSE, a difference in convergence is detected. Aside from the errors in the numerical solution for the BE, regarding the polarization, the boomeron- and trappon behaviour is much more distinct for the BE then for the NLSE. The reason for this is probably the lack of second order derivatives and third order terms in the numerical solution for the BE.

Chapter 4

Summary and Conclusions

This report present an in-depth analysis of the boormeon and trappon phenomena for the BE and the NLSE. These phenomena emerges as solition solutions to a number of nonlinear differential equations, presented in this report. An analytical and numerical analysis have been conducted for the BE, a special case of the generalized KdV, and the NLSE. The analytical solutions for the BE have been derived with the inverse scattering transform (IST) technique and the analytical solution for the NLSE has also been presented.

The analytical solution of the BE presented in this report is more detailed than the corresponding solutions found in previous papers. This detailed description explains the connection between the polarization of the solution and the changing velocity. The analytical solution of the NLSE is also described thoroughly, containing a physical interpretation of the two components enabling a comparison between the solution for the BE and the solution for the NLSE. The polarization-velocity connection has been in focus. When comparing the two solutions it was found that, using the introduced physical interpretation for the NLSE, the polarization-velocity connection described for the BE is applicable on the NLSE. This interesting conclusion shows that both boomeron solutions, of the BE and the NLSE, have the same asymptotic behaviour for $t \to \pm\infty$ regarding the polarizations. The behaviour of the polarization for the two solutions in the intermediate time is also very similar. Similarities for the trappon solutions, between the BE and the NLSE, have also been demonstrated. Both solutions have an oscillating polarization giving rise to the oscillating velocity, characteristic for the trappon solutions. The main difference for the two solutions is the number of dimensions in which the polarization trajectories take place. For the scalar single-soliton solutions for the two equations, one the other hand, the resemblence in both the mathematical expressions and the plots is striking.

The numerical analysis for the BE and the NLSE was performed with the help of the software program MATLAB. The analysis was implemented using the FDM. For comparison, the analytical and numerical solutions have been simulated respectively, with the same parameters.

For the BE an error still remains in the written programs. The numerical solutions did, however, exhibit bommeron behaviour but for different values of the parameters in the BE. The numerical solution did also exhibit trappon behaviour. The trappon behaviour was found for the same values as the trappon solutions to the analytical solutions but differed slightly in the single-soliton solution. The error has been investigated using the

introduced way of displaying the polarization for the solutions. The polarization for the trappon solutions differed significantly. This investigation of the polarization resulted in the conclusion that two solutions, with strong similarities for the single-soliton solution, can have very different polarization trajectories.

For the NLSE the difference between the analytical solutions and the numerical solutions is significant. The reasons, most likely, for this are the number of FDM approximations needed, the second order derivative in the simulation and the terms of order three. Nevertheless, the emerging of the boomeron- and trappon properties for the numerical simulation of the NLSE is clear.

To Summarize the numerical analysis, an interesting aspect of these calculations is that, with a rather simple numerical model for these complex equations, it is possible to obtain boomeron- and trappon solitons. However, a problem with the divergence when using the simple FDM model have occurred when setting too rough or too small descretisations for h and t_s. This of course is a drawback of the model, but after testing different discretizations and different parameters for the equations, the divergence ultimately was avoided.

One aspect not treated in this report is the possibility of two different polarization trajectories having the same scalar single-soliton solution for the BE. This only regards the BE since the dimensions for the NLSE does not allow this freedom. For the BE this might be possible since the position, $\xi(t)$, and thereby the velocity, depend solely on the introduced scalar $S(t)$. The scalar, $S(t)$, in turn, is closely connected to the vector $\boldsymbol{S}(t)$ determening the polarizarion $\hat{\boldsymbol{n}}(t)$.

Bibliography

[1] T. Aktosun, *Inverse Scattering Transform and the Theory of Solitons*, Enc. of Compl. and Syst. Sci., R. A. Meyers (ed.), Springer, New York, pp. 4960-4971, (2009)

[2] F. Calogero and A. Degasperis, *New Integrable Equations of Nonlinear Schrödinger Type*, Studies in Applied Mathematics, Vol **113(1)**, pp. 91-137, (2004)

[3] F. Calogero and A. Degasperis, *Coupled Nonlinear Evolution Equations Solvable Via the Inverse Spectral Transform, and Solitons that Come Back: the Boomeron*, Lett Nuovo Cimento, Vol **16**, N **14**, (1976)

[4] F. Calogero and A. Degasperis, *Nonlinear Evolution Equations Solvable by the Inverse Spectral Transform. - I*, Il Nuovo Cimento, Vol **32**, N **2**, (1976)

[5] F. Calogero and A. Degasperis, *Nonlinear Evolution Equations Solvable by the Inverse Spectral Transform. - II*, Il Nuovo Cimento, Vol **19**, N **1**, (1977)

[6] F. Calogero ed. and A. Degasperis, *Nonlinear evolution equations solvable by the spectral transform*, Re. Notes in Math., Pitman, pp. 97-126, (1978)

[7] F. Calogero, A. Degasperis and S. De Lillo, *The multicomponent Eckhaus equation*, J. Phys. A: Math. Gen, **30**, pp. 5805-5814, (1997)

[8] A. Degasperis, *Integrable models in nonlinear optics and soliton solutions*, J. Phys A: Math Theor. **43** 434001, (2010)

[9] A. Degasperis, M. Conforti, F. Baronio and S. Wabnitz, *Effects of nonlinear wave coupling: Accelerated solitons*, Eur. Phys. J. Special Topics **147**, pp. 233-252, (2007)

[10] F. Demontis, *Direct and Inverse Scattering of the Matrix Zakharov-Shabat system*, Ph.D. report, Università di Cagliari, (2006)

[11] P.G. Drazin and R.S. Johnson, *Solitons: an introduction*, Cambrige University Press, Applied Mathematics, (1989)

[12] Torbjörn Erikson et al., *Fysikens matematiska metoder*, Department of Theoretical Physics, Royal Institute of Technology (KTH), (1997)

[13] C. S. Gardner, J. M. Greene, M. D. Kruska and R. M. Miura, *Method for Solving the Korteweg-de Vries equation*, Phys. Rev. Lett. **19**, pp. 1095-1097, (1967)

[14] P. Lax, *Integrals of Nonlinear Equations of Evolution and Solitary Waves*, Commun. Pure Appl. Math. **21**, pp. 467–490, (1968)

[15] S. V. Manakov, *On the theory of two-dimensional stationary self-focusing of electromagnetic waves*, Zh. Eksp. Tecr. Fiz. **65**, pp. 505-516, (1973)

[16] S. C. Mancas and R. S. Coudhury, *trappon solitons in the cubic–quintic Ginzburg–Landau equation* , Mathematics and Computations in Simulation, **80**, pp. 73-82, (2009)

[17] R. S. Palais, *An Introduction to Wave Equations and Solitons*, The Mordningside Center of Mathematics, Chinese Academy of Science, Beijing, (2000)

[18] M. Remoissenet, *Waves Called Solitons: Concepts and Experiments*, Springer Verlag, (1999)

[19] C. Sulem and P.L. Sulem, *The Nonlinear Schrödinger Equation*, Applied Mathematical Sciences, Vol **139**, Springer-Verlag, Berlin, 1999.

[20] L. Yun and D. Han *Evolution of dual-wavelength fiber laser from continuous wave to soliton pulses*, Optics Communications **285**, pp. 5406-5409, (2012)

[21] V. E. Zakharov and A. B. Shabat, *Exact theory of two-dimensional self-focusing and one-dimensional self-modulation of waves in nonlinear media*, Sov. Phys. JETP. **34**, pp. 62-69, (1972)

Appendix A

A.1 Derivation of the Lax Pair Equation

The Lax pair equation is treated in Sec. 3.3.1. A derivation of this equation now follows. One will solve the following eigenvalue problem $L\psi = \lambda\psi$ and $\psi_t = P\psi$, with the restriction that the spectral parameter, λ is invariant in time, i.e. $\lambda_t = 0$. L and P are two linear operators. One starts by deriving $L\psi = \lambda\psi$ with respect of time

$$L_t\psi + L\psi_t = \lambda_t\psi + \lambda\psi_t. \tag{A.1}$$

Having $\psi_t = P\psi$ and $\lambda_t = 0$ one gets

$$L_t\psi + LP\psi = \lambda P\psi. \tag{A.2}$$

Due to the fact that λ is an eigenvalue, thus a constant, one can also let P operate on λ as well. Thus by rearranging the equation the following expression is obtained

$$\begin{aligned} L_t\psi + LP\psi = P(\lambda\psi) = PL\psi, \\ \Rightarrow (L_t + LP - PL)\psi = 0. \end{aligned} \tag{A.3}$$

Since $\psi \neq 0$, finally one get the Lax pair equation, Eq. (3.1),

$$\begin{aligned} 0 = L_t + LP - PL = L_t - [P, L] \\ \Rightarrow L_t = [P, L]. \end{aligned} \tag{A.4}$$

However, finding a Lax pair that corresponds to a given nonlinear differential equation is cumbersome, involving some intuitive mathematical guessing by the seeker [14].

A.2 Generalized Polarization Expressions for the Nonlinear Schrödinger Equation

In this section the most general expressions for the NLSE polarizations $A^{(1)}(t)$ and $A^{(2)}(t)$ are displayed. The expressions include both the sinh- and cosh terms and the sinusoidal terms giving a deeper understanding of the NLSE solution.

$$\begin{aligned} A^{(1)}(t) = -2a \cdot [S(t)]^{-1/2} \{\sinh[\zeta t + \nu]\cos[\delta t + \tau] + \\ i\cosh[\zeta t + \nu]\sin[\delta t + \tau]\}\, e^{i\left(p^2 - k^2\right)t}, \end{aligned} \tag{A.5}$$

$$A^{(2)}(t) = 2 \cdot [S(t)]^{-1/2} \Bigg\{ \sqrt{b^2 (p-ik)^2 - |a|^2} \Bigg(\cosh[\zeta t + \nu] \cos[\delta t + \tau] + i \sinh[\zeta t + \nu] \sin[\delta t + \tau] \Bigg) - b(p-ik) \Bigg(\sinh[\zeta t + \nu] \cos[\delta t + \tau] + i \cosh[\zeta t + \nu] \sin[\delta t + \tau] \Bigg) \Bigg\} e^{i(p^2 - k^2)t}. \tag{A.6}$$

A.3 Numerical Expressions for the Boomeron Equation

Here is the FDM approximation of the BE, needed when doing the numerical analysis in Sec. 3.4.1. The following expressions are obtained when using central difference in both the spatial and temporal dimensions

$$u_{x,i,j+1} = u_{x,i,j-1} + 2t_s \cdot \left\{ b_1 \frac{v^{(1)}_{x,i+1,j} - v^{(1)}_{x,i-1,j}}{2h} + b_2 \frac{v^{(2)}_{x,i+1,j} - v^{(2)}_{x,i-1,j}}{2h} + b_3 \frac{v^{(3)}_{x,i+1,j} - v^{(3)}_{x,i+1,j}}{2h} \right\}, \tag{A.7}$$

$$v^{(1)}_{x,i,j+1} = v^{(1)}_{x,i,j-1} + 2t_s \cdot \left\{ b_1 \frac{u_{x,i+1,j} - u_{x,i-1,j}}{h^2} + \left(a_2 v^{(3)}_{x,i,j} - a_3 v^{(2)}_{x,i,j} \right) - 2 \left(v^{(2)}_{x,i,j} \cdot w^{(3)}_{i,j} - v^{(3)}_{x,i,j} \cdot w^{(2)}_{i,j} \right) \right\}, \tag{A.8}$$

$$v^{(2)}_{x,i,j+1} = v^{(2)}_{x,i,j-1} + 2t_s \cdot \left\{ b_2 \frac{u_{x,i+1,j} - u_{x,i-1,j}}{h^2} + \left(a_3 v^{(1)}_{x,i,j} - a_1 v^{(3)}_{x,i,j} \right) - 2 \left(v^{(3)}_{x,i,j} \cdot w^{(1)}_{i,j} - v^{(1)}_{x,i,j} \cdot w^{(3)}_{i,j} \right) \right\}, \tag{A.9}$$

$$v^{(3)}_{x,i,j+1} = v^{(3)}_{x,i,j-1} + 2t_s \cdot \left\{ b_3 \frac{u_{x,i+1,j} - u_{x,i-1,j}}{h^2} + \left(a_1 v^{(2)}_{x,i,j} - a_2 v^{(1)}_{x,i,j} \right) - 2 \left(v^{(1)}_{x,i,j} \cdot w^{(2)}_{i,j} - v^{(2)}_{x,i,j} \cdot w^{(1)}_{i,j} \right) \right\}, \tag{A.10}$$

$$w^{(1)}_{x,i+1,j} = w^{(1)}_{x,i-1,j} + 2h \left\{ b_3 v^{(2)}_{x,i,j} - b_2 v^{(3)}_{x,i,j} \right\}, \tag{A.11}$$

$$w^{(2)}_{x,i+1,j} = w^{(2)}_{x,i-1,j} + 2h \left\{ b_1 v^{(3)}_{x,i,j} - b_3 v^{(1)}_{x,i,j} \right\}, \tag{A.12}$$

$$w^{(3)}_{x,i+1,j} = w^{(3)}_{x,i-1,j} + 2h \left\{ b_2 v^{(1)}_{x,i,j} - b_1 v^{(2)}_{x,i,j} \right\}. \tag{A.13}$$

However, when setting $j = 1$ and $i = 1$, in the above expressions, forward difference, instead of central difference, have to be calculated for both the temporal and spatial dimensions respectively, due to the fact that the components with indices $j - 1 = 0$ and

$i-1=0$, do not exists. Consequently for the time derivative, with forward difference, one gets

$$\begin{aligned} u_{xt}(x_i,t_1) &= \frac{u_{x,i,2}-u_{x,i,1}}{h} \\ \Rightarrow u_{x,i,2} &= u_{x,i,1}+h\cdot u_{xt}(x_i,t_1), \end{aligned} \tag{A.14}$$

which is computed analogiously for each expression in Eq. (A.8) through Eq. (A.10) respectively. Further, when setting $i=n$ in Eq. (A.8) through Eq. (A.13), the use of backward difference is required for the approximations of the spatial derivatives. To give an example of backward difference, the $u_{xx}(x,t)$ term in Eq. (A.8) thorough Eq. (A.10) is computed in terms of $u_x(x,t)$

$$\begin{aligned} u_{xx}(x_n,t_j) &= \frac{u_{x,n,j}-u_{x,n,j}}{h} \\ \Rightarrow u_{x,n,j} &= u_{x,n,j}+h\cdot u_{xx}(x_i,t_1). \end{aligned} \tag{A.15}$$

Consequently, a numerical algorithm for the time evolution of the BE, Eq. (2.5), has been executed.

A.4 Numerical Expressions for the Nonlinear Schödinger Equation

The FDM approximation of the NLSE, from Sex.3.4.2, with the use of central difference in both the spatial and temporal dimension, are as follow,

$$\begin{aligned} u^{(1)}_{i,j+1} = u^{(1)}_{i,j-1} + 2t_s \Bigg\{ & -au^{(2)}_{i,j+1} + b\frac{u^{(1)}_{i+1,j}-u^{(1)}_{i-1,j}}{2h} + w_{i,j}u^{(2)}_{i,j} \\ & +i\left[\frac{u^{(1)}_{i+1,j}+u^{(1)}_{i-1,j}-2u^{(1)}_{i,j}}{h^2} + 2\left(\left|u^{(1}_{i,j}\right|^2 + \left|u^{(2)}_{i,j}\right|^2\right)u^{(1)}_{i,j}\right]\Bigg\}, \end{aligned} \tag{A.16}$$

$$\begin{aligned} u^{(2)}_{i,j+1} = u^{(2)}_{i,j-1} + 2t_s \Bigg\{ & a^*u^{(1)}_{i,j+1} - b\frac{u^{(2)}_{i+1,j}-u^{(2)}_{i-1,j}}{2h} - w^*_{i,j}u^{(1)}_{i,j} \\ & +i\left[\frac{u^{(2)}_{i+1,j}+u^{(2)}_{i-1,j}-2u^{(2)}_{i,j}}{h^2} + 2\left(\left|u^{(1)}_{i,j}\right|^2 + \left|u^{(2)}_{i,j}\right|^2\right)u^{(2)}_{i,j}\right]\Bigg\}, \end{aligned} \tag{A.17}$$

$$w_{i+1,j} = w_{i-1,j} + 4hb\cdot u^{(1)}_{i,j}u^{(2)*}_{i,j}. \tag{A.18}$$

Eq. (A.16) through Eq. (A.18) can be used to determine $u^{(1)}_{i,j}$ and $u^{(2)}_{i,j}$ when $2<i<(n-1)$ and $3<j<m$. Fortunately, $i=1$ and $i=n$ have already been set by the boundary condition. To compute $u^{(1)}_{i,j=2}$ and $u^{(2)}_{i,j=2}$ it is necessary to use forward difference, instead of central difference, in the temporal dimension.